Carbon-13 Nuclear Magnetic Resonance Spectroscopic Studies of ^{13}CO Adsorbed on Platinum Particles in L-Zeolites

Oc Hee Han*, Gustavo Larsen†,# Gary L. Haller†, and Kurt W. Zilm‡

Magnetic Resonance Research Group, Korea Basic Science Institute, Taejon 305-333, Korea
†Departments of Chemistry and ‡Chemical Engineering, Yale University, New Haven, CT 06511, U.S.A.
Received March 12, 1998

^{13}CO chemisorbed on platinum particles in L-zeolite has been investigated by static and magic angle spinning NMR spectroscopy. The representative spectra are composed of a broad asymmetric peak with a center of gravity at 230±30 ppm and a sharp symmetric peak at 124±2 ppm which is tentatively assigned to physisorbed CO_2 on inner walls of L-zeolite. Overall, the broad resonance component is similar to our previous results of highly dispersed (80-96%) CO/Pt/silica or CO/Pt/alumina samples, still showing metallic characters. The principal difference is in the first moment value. The broad peak in the spectra is assigned to CO linearly bound to Pt particles in the L-zeolites, and indicates a distribution of isotropic shifts from bonding site to bonding site. The NMR results reported here manifest that the Pt particles inside of the L-zeolites channels are not collectively the same with the ones supported on silica or alumina with similar dispersion in terms of Pt particle shape and/or ordering of Pt atoms in a particle. As a result, Pt particles of CO/Pt/L-zeolite were agglomerated accompanying CO desorption upon annealing. There were no definite changes in the NMR spectra due to differences of exchanged cations. Comparison of our observation on CO/Pt/L-zeolite with Sharma *et al.'s* reveals that even when the first moment, the linewidth, and the relaxation times of the static spectra and the dispersion measured by chemisorption are similar, the properties of Pt particles can be dramatically different. Therefore, it is essential to take advantage of the strengths of several techniques together in order to interpret data reliably, especially for the highly dispersed samples.

Introduction

^{13}C nuclear magnetic resonance (NMR) studies have been especially informative on the nature of the bonding of CO to transition metals on supported catalysts.[1-11] The Knight shift of the ^{13}C resonance provides a measure of the involvement of the metal's conduction electrons in the chemical bond between the metal surface and adsorbate.[1-13] Line shapes in the ^{13}C spectra for ^{13}CO on these metals are quite broad[8,13] due to the demagnetizing field of the metal particles and a wide site-to-site variation in the isotropic shift when the metal particles are sufficiently big enough to have metallic characters.

When the metal particles are smaller, they are expected to lose metallic characters. This phenomenon was observed with ^{13}C NMR of CO adsorbed on highly dispersed (dispersion-100%) silica supported Rh or Ru particles.[6,7a] The first moment (M_1) of the line shape was not Knight shifted anymore and spin-lattice relaxation times became too long to be due to conduction electrons.[6,7,10] Magic angle spinning (MAS) could narrow the overall line shape dramatically producing center peaks for the linearly bonded CO and multicarbonyls and accompanying spinning side bands; the bridging CO peak was not sufficiently narrowed to be observed in the MAS spectra.[7a]

Reduction of M_1 and diffusion on the surface of Pd particles for the highly dispersed (56%) Pd samples was observed when compared with the low dispersion Pd samples.[2] However, MAS was not effective to bring any change to the line shape of ^{13}CO on highly dispersed Pd sample which still shows metallic character by Knight shift and short T_1 relaxation time.[2] Carbon monoxides on colloidal Pd particles of 20±3 Å diameter were reported to have an inhomogeneously broadened linewidth and a small M_1 (190 ppm).[14] On the other hand, ^{13}C NMR spectra of CO on silica or alumina supported Pt particles were independent of dispersion (between 11% and 80-96%)[1,12,13] and not effectively narrowed by MAS.[1]

There are several reasons why L-zeolite was chosen as a support material for the experiments. The metal particle size is expected to be regulated by the sizes of the channels of the L-zeolites. L-zeolite has a structure of parallel channels.[16] The throat diameter of a channel is about 12 Å. If there is a metal-support interaction, it may be more pronounced within a zeolite because the particle in the channels may interact with the zeolite over a substantial fraction of its surface. Also, the interaction in basic L-zeolite supported samples is expected to be different from that in the samples supported on acidic materials like alumina.[17-19]

While this paper was in preparation, the ^{13}C NMR study on ^{13}CO adsorbed on highly dispersed (87%) Pt particles in L-zeolites was published independently by Sharma *et al.*[15] Their static ^{13}C spectra are similar to ours in terms of line shape and M_1 values. However, their MAS results and T_1 data interpretation were not consistent with our results. In this report, our ^{13}C NMR data for ^{13}CO adsorbed on highly dispersed Pt particles in L-zeolites are presented and interpreted in comparison with Sharma *et al.'s*.

#Present address: Department of Chemical Engineering, University of Nebraska Lincoln, Nebraska 68588, USA
*To whom all correspondence should be addressed.

Experimental

Sample preparation. A stirred suspension of 1 g potassium L-zeolite (1 g zeolite/100 ml water) was ion exchanged with a desired amount of $Pt(NH_3)_4(NO_3)_2$ salt for 24 hours. The precursor was filtered, washed, and dried at 80 for 3-4 hours. After drying, the precursor was oxidized and reduced in an U-tube Pyrex reactor in the following way: i) 100 mL/min of pure oxygen was passed through the precursor while increasing the temperature from 25 °C to 350 °C in 5 hours. ii) the oxygen was purged with helium at 350 °C for 15 min. iii) the reduction step was carried out at 350 °C for 2 hours under 100 mL/min hydrogen flow. The reduced sample was back-exchanged with a 0.3 M solution of the desired cation nitrate (in our case, Mg^{++}, Ca^{++}, or Ba^{++}) at room temperature for 72 hours in a ratio of 1 g zeolite/100 mL solution. The catalyst was filtered, washed, dried at 80 for 3-4 hours, and finally rehydrated to constant weight for storage. The weight percentages of platinum in the samples were 3.58, 3.45, and 3.50 for Pt/MgL, Pt/CaL, and Pt/BaL catalysts, respectively. From here on, ML designates M^{++} ion exchanged L-zeolite.

Just before the CO adsorption step, the samples were activated under hydrogen atmosphere at 320 °C for 45 min and outgassed at the same temperature for half an hour. About 150 mg of catalyst were placed in the 5 mm NMR tubes. The catalyst was exposed to ^{13}CO (99.7%, MSD isotopes) at a pressure of 12 Torr (1 Torr=133.3 N/m^2) at room temperature for a total of 10 min. After chemisorption the catalysts were evacuated for 30 min at room temperature to remove gas phase CO. The tubes were then sealed with a torch at about 4.5 cm length. During the sealing procedure the sample temperature never exceeded 70 °C. Volumetric chemisorption indicated that dispersions measured by hydrogen were 1.05, 1.06, and 1.05 and that adsorption CO/H ratios were 0.90, 0.79, and 0.74 for CO/Pt/MgL, CO/Pt/CaL, and CO/Pt/BaL samples, respectively. Extended X-ray absorption fine structure (EXAFS) data taken on the catalysts prior to back-exchange, gave an average coordination number, N=6.5, which matched with hydrogen chemisoption data before and after divalent cation back-exchange. Therefore, the Pt particle sizes were not affected by the back-exchange process and the average diameter of the particles was 10-12 Å.

Annealing was carried out by putting the sealed tube into the mineral oil bath at 175±3 °C for 18±0.2 hours (for CO/Pt/CaL) or into the preheated oven at 174±3 °C for 15±0.2 hours (for CO/Pt/BaL). The samples were cooled down to room temperature within 5 min in ambient air. The blank samples were prepared by degassing either after activating Pt/BaL or Pt/CaL, or after exposing CaL to ^{13}CO gas.

Nuclear Magnetic Resonance Spectroscopy. Experiments were carried out at field strengths of 2.35, 7.05, and 11.7 T. The low field system has a proton frequency of 100.014 MHz, and is equipped with a Nicolet data system and an Oxford Instruments wide-bore (89 mm) superconducting solenoid. The middle field system operates at a proton frequency of 300.8 MHz and is equipped with a Tecmag data system and an Oxford Instruments wide-bore superconducting solenoid. The high field instrument, a Bruker AM-500 spectrometer, has 500.13 MHz for proton frequency and a standard-bore (52 mm) superconducting magnet.

The MAS probes for 2.35 and 7.05 T use a rotor similar to one described by Gay.[20] The sample cells fit snugly in torlon rotors and typically spin between 2.0 and 2.5 kHz. The MAS spin rate was measured before and after each run electronically. Variable temperature experiments were done with a static dewared probe at 80 K and 388 K and at 7.05 T.

In all experiments, spin echo sequences and phase cycling of the pulses were used to suppress pulse breakthrough and other artifacts.[21] The separation τ between the $\pi/2$ pulse and the τ pulse in the spin echo was typically 30-50 μs for the high and middle field instruments and 170 μs for the low field instrument. For MAS, a spin echo with π pulse timed to occur exactly one rotor period after the initial $\pi/2$ pulse was employed at the middle and low fields. If the echo sequence is not synchronous with the sample rotation, the MAS can interfere the spin echo resulting in destruction of the echo signal.[22,23] Room temperature static spectra on the middle and low field instruments typically required over 4000 and 20,000 accumulations, respectively. All echo signals were acquired in quadrature with the carrier placed close to the resonance's center of gravity. Line shapes were checked for independence of resonance offset and background spectra. Since the phasing of powder spectra can be quite subjective if there are no well-defined features present, zeroth order phasing was determined using the powder pattern from 10% ^{13}C enriched $BaCO_3$. A typical $\pi/2$ pulse length for the hard pulse was 2.5-4.5 μs and a pulse program repetition rate of 4-5.5 s was employed unless stated otherwise.

For the hole burning experiments,[24-26] the ^{13}C spins were first prepared by irradiation with a multiple-pulse approximation to a soft Gaussian-shaped pulse.[25,26] A 24-pulse sequence was used with a 45 μs $\pi/2$ pulse length and the gap between each soft pulse was 30 μs. Then, a spin echo sequence was applied to detect the remaining magnetization after a variable delay τ_D.

Total suppression of spinning sidebands (TOSS)[27-30] and phase-altered spinning sidebands (PASS)[27] techniques were used to acquire centerband-only spectra and spectra with all odd order spinning sidebands inverted, respectively. The performance of the four pulse TOSS sequence[28,29] and the PASS pulse sequence was checked with a highly dispersed CO/Rh/silica sample.[7] Chemical shifts reported here are all relative to external neat tetramethylsilane (TMS) with downfield shifts taken as positive and have a precision of about 1 ppm unless stated otherwise.

Results

The representative ^{13}C spectra (Figure 1) were composed of a broad asymmetric peak with a center of gravity at 230±30 ppm and a sharp symmetric peak at 124±2 ppm. The overall line shape on a ppm scale was the same at all three magnetic field strengths. However, the percentages of the sharp peaks differed slightly from sample to sample (Ca; 9%, Mg and Ba; 2%). These percentages have increased very slowly (from 2 to 4% and 9 to 17%) when the samples were aged for several years.

MAS did not narrow the broad peak (Figure 2B). Also, this spectrum had some signal loss compared to the static spectrum (Figure 1C) with 30-50 μs τ values due to T_2 distortion caused by long τ values corresponding to a rotor

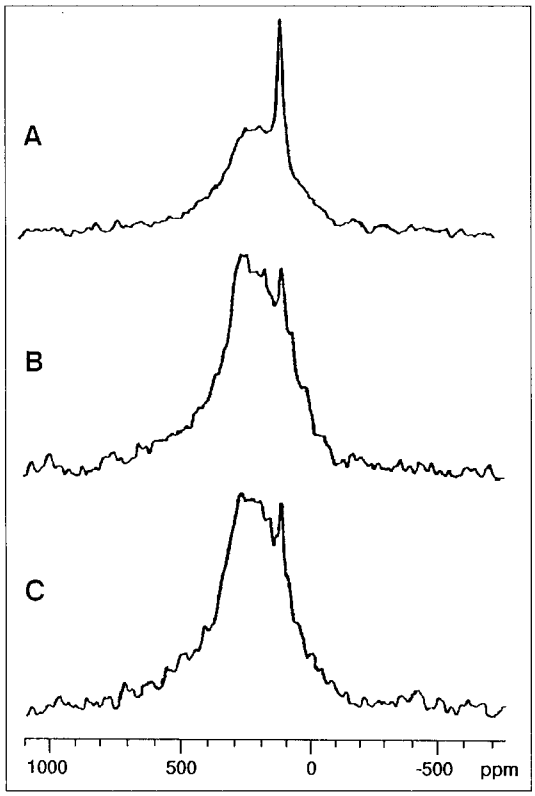

Figure 1. ^{13}C static echo spectra of (A) CO/Pt/CaL, (B) CO/Pt/MgL, (C) CO/Pt/BaL at 7.05 T with τ = 30 μs.

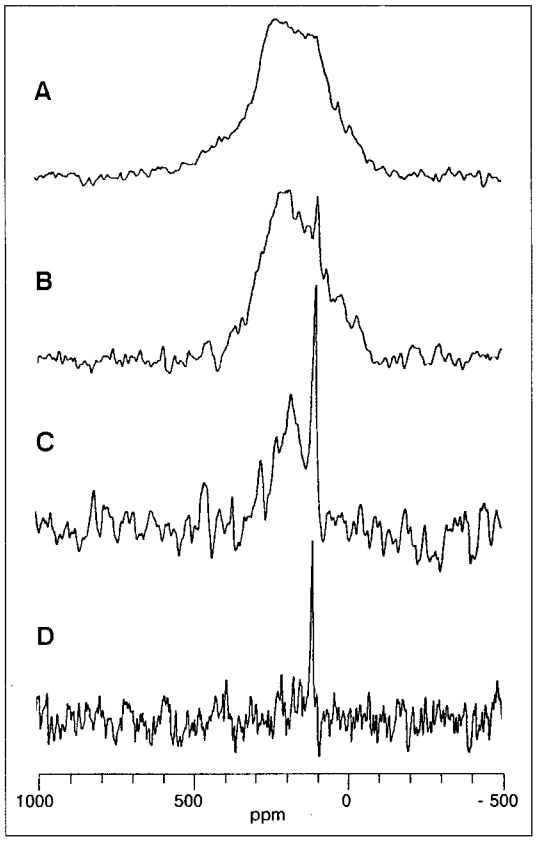

Figure 2. ^{13}C (A) static echo spectrum with τ=435 μs and (B) MAS echo spectrum of CO/Pt/BaL at 2.3 kHz spinning speed and 7.05 T. (C) TOSS spectrum of CO/Pt/BaL at 2.2 kHz spinning speed and 7.05 T. (D) PASS spectrum of CO/Pt/BaL at 7.05 T and 2.2 kHz spinning speed.

period. The MAS spectrum (Figure 2B) had a little change of line shape from that of the static spectrum (Figure 2A) with the same τ value.

Since the linewidth of the spectra shown in Figure 1 is greater than the sample spinning frequency, the lack of any narrowing under MAS can simply be the result of having a wide distribution of isotropic shifts. To investigate this possibility TOSS and PASS spectra were acquired. Four pulse TOSS spectra were taken at 2.35 and 7.05 T magnetic field strengths. Representative TOSS and PASS spectra are shown in Figure 2C and 2D. Unfortunately, the TOSS spectra had a very poor signal-to-noise ratio due to the short T_2 of the samples and the inherent intensity loss of TOSS technique. It is well known that the peak intensity of TOSS spectra is smaller as the ratio of the static linewidth of the chemical shift anisotropy pattern to spinning speed is greater.[30] This ratio, on the contrary, is not supposed to affect the intensities in PASS spectra.[27] The linewidths of TOSS spectra were about half of those from static or MAS spectra for a given spinning rate, and only a sharp peak at 124 ppm was observed in the PASS spectrum.

The M_1 of the broad line was observed to remain unchanged at 80±3 K, and the sharp peak was broadened at this temperature (Figure 3A). The M_1 of total line shape at this temperature was regarded as that of the broad peak since the relative intensity of 124 ppm peak was only about 2% of the total signal intensity. The spectrum taken at 388 K (not shown) was the same as that at room temperature within experimental error.

Diffusion of the CO at room temperature was studied using a hole burning technique and a low temperature ex-

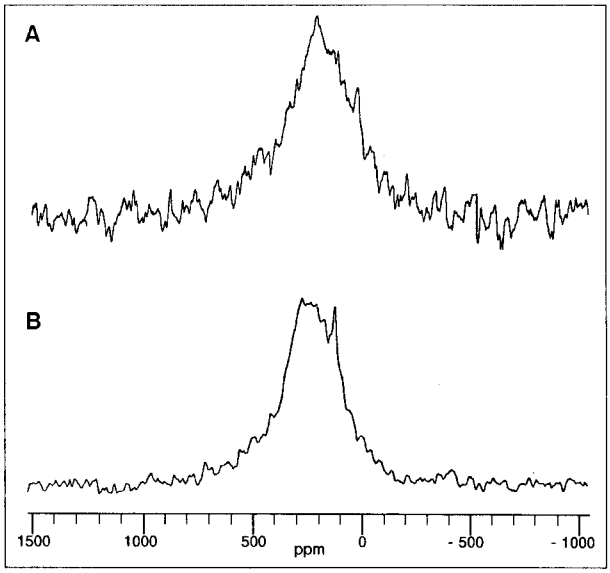

Figure 3. ^{13}C static echo spectra of CO/Pt/BaL (A) at 77 K and (B) at room temperature.

periment (Figure 3A) at 75 MHz. Experimentally measured half-widths of the holes were 1.0±0.3 kHz. The shape of the hole spectra did not depend on τ_D for several positions in the line shape and always was found to decay at the same rate with T_1.

The samples were also characterized by their T_1's and T_2's at 7.05 and 11.4 T and room temperature. An inversion recovery followed by a spin echo was used in the T_1 determination (Figure 4). The T_2's were also determined with a standard spin echo sequence. Relaxation times, T_1 and T_2, were anisotropic and increased as one moved from low to high field positions in the line shape. T_1's ranged from 70 ms to 420 ms from the inversion recovery null points along the resonance frequency positions from 400 ppm to 100 ppm in the line shape. The T_1 data points at any given frequency did not fit a single exponential (Figure 5) while the T_2 data points did. T_2's had a range from 800± 100 μs to 1.2±0.4 ms along the resonance frequency positions from 400 ppm to 100 ppm. The T_1 and T_2 relaxation times were the same at 7.05 and 11.7 T (Figure 5). If an average T_1 over the line shape is taken from the null area point of the inversion recovery data, the product of temperature (295 K) and T_1 is 64±10 Ks for CO/Pt/L-zeolite samples. This is to be compared with 40±6 Ks (from our previous publication)[1] or 46±3 Ks (from Slichter's data)[9] for CO/Pt/silica or CO/Pt/alumina samples. Our T_1 data could be well fitted with three exponential functions as Sharma *et al.'s*. For example, 250 ppm point of ^{13}C inversion recovery spectra of CO/Pt/CaL obtained at 7.05 T was fitted with 35±8% for T_1=50±20 ms, 45±20% for T_1=650±320 ms, and 20±12% for T_1=6.6±5.2 s (Figure 5). Sharma *et al.* obtained 14±2% for T_1=800±600 ms, 50±3% for T_1= 1.5±0.3 s, and 36±4% for T_1=6.6±1.6 s from ^{13}C saturation recovery spectra of CO/Pt/KL at 7.05 T.

After annealing, there was dramatic change in the spectrum (Figure 6B) which was compared with the one before annealing (Figure 6A). Three peaks relaxing at different

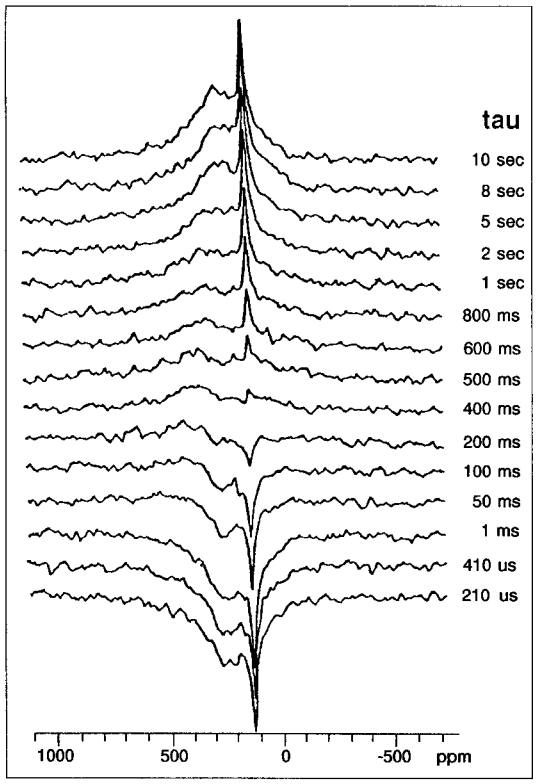

Figure 4. Inversion recovery spectra of CO/Pt/CaL at 7.05 T.

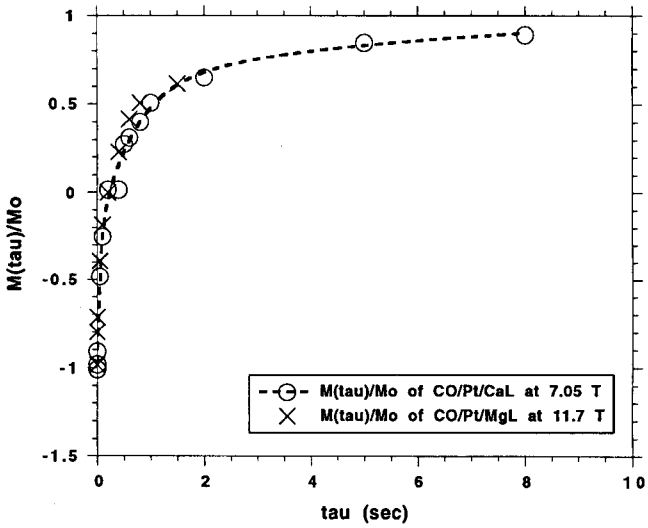

Figure 5. A plot of M/M_0 versus τ of inversion recovery at 250 ppm. The data points were taken from CO/Pt/MgL at 11.7 (X) and from CO/Pt/CaL at 7.05 T(O). The dashed line is a fit with three exponentials: 35 8% for T_1=50±20 ms, 45±20% for T_1= 650±320 ms, and 20±12% for T_1=6.6±5.2 s.

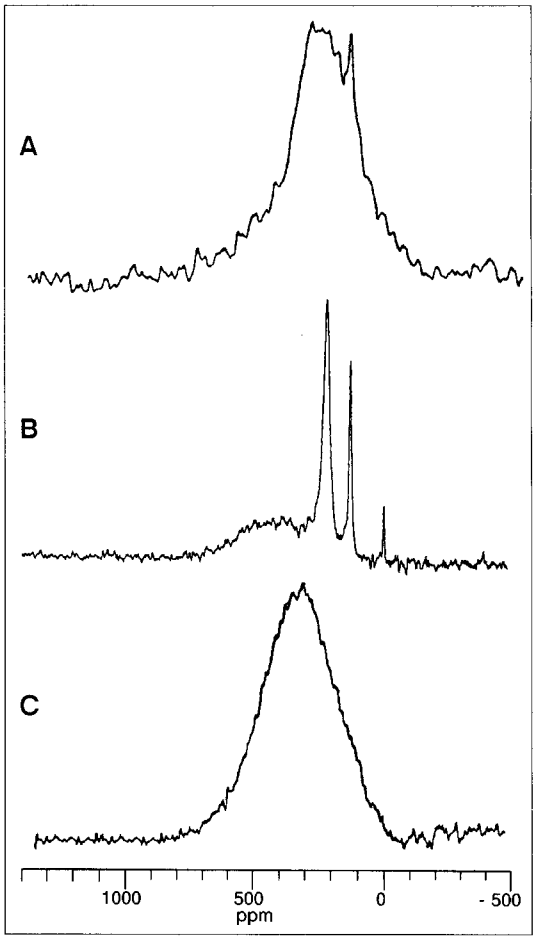

Figure 6. ^{13}C static echo spectra of the CO/Pt/BaL at 7.05 T (A) before and (B) after annealing. (C) ^{13}C static echo spectrum of the CO/Pt/alumina at 7.05 T and room temperature.

rates appeared in the spectra of the annealed samples. The relaxation rates of each peak at 7.05 and 11.74 T were

Table 1. Relaxation data of the annealed CO/Pt/BaL sample at 7.05 and 11.7T

M_1	T_1		T_2	
	7.05T (ms)	11.7T (ms)	7.05T (μs)	11.7T (μs)
340±30 ppm	1.3×10^2	1.0×10^2	4.5×10^2	3×10^2
210±10 ppm	2.0	2.4	1.7×10^2	6×10^1
124±2 ppm	5.6×10^2	6.5×10^2	6.3×10^2	2×10^2
181±1 ppm	0.39	No data	3.0×10^2	No data

summarized in Table 1. The broad peak at 340±30 ppm has the similar overall line shape (Figure 6C), first moment, and relaxation behavior to the one of CO/Pt/alumina or silica previously reported.[1,12,13] The line shape of the peak at 340±30 ppm[1,12] was a little deviated from a Gaussian shape. The peaks at 210±10 ppm and 124±1 ppm had Lorentzian line shapes; the widths were homogeneous and governed by T_2 relaxation. The representative inversion recovery spectra of the annealed CO/Pt/BaL were shown in Figure 7. The relaxation times (T_1~560 ms and T_2~630 μs) of the 124 ppm peak of the CO/Pt/BaL sample after annealing at 174±3 °C were the same as those of the sample before annealing. The only gas phase CO peak, which wasn't observed before annealing, was detected at 181±1 ppm (Figure 8A) from the vacant portion of the sample tube. The peak at 124±2 ppm

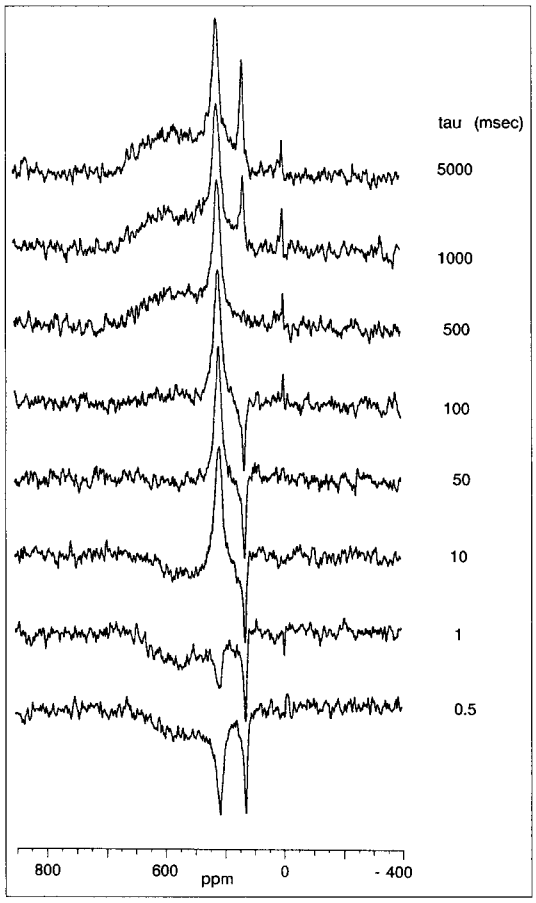

Figure 7. The inversion recovery spectra of the annealed CO/Pt/BaL at 7.05T.

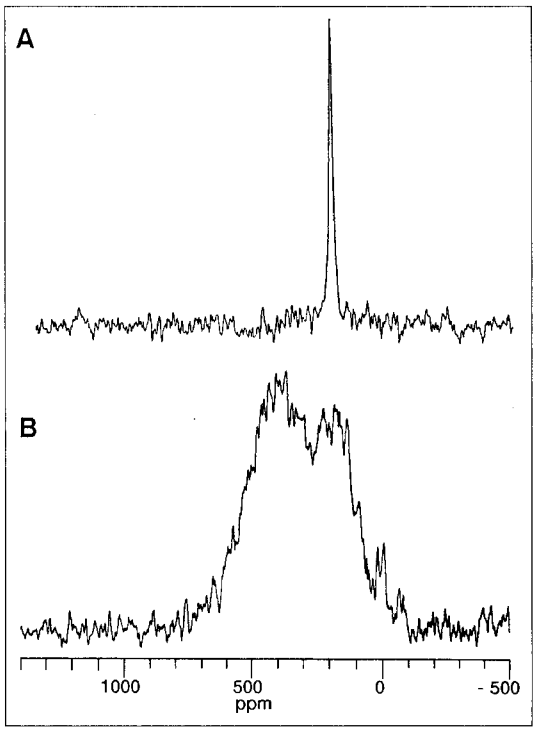

Figure 8. (A) ^{13}C static echo spectrum of the vacant portion of the annealed CO/Pt/CaL at 7.05 T. (B) ^{13}C static echo spectrum of the annealed CO/Pt/BaL at 7.05 T and -160±3 °C.

was not present in the spectrum of the vacant portion of the sample tube before and after annealing. The peaks at 210± 10 ppm and at 124±1 ppm were broadened in the low temperature spectra (Figure 8B). The spectral change upon annealing was similar for CO/Pt/BaL and CO/Pt/CaL samples except negligible relative intensity variation of peaks as shown in Table 2, which could be just attributed to difference of annealing duration. The remained peak intensity after subtraction of the area of the peaks at 210±10 and 124±1 ppm from the total resonance signal was taken as the intensity of the 340±30 ppm peak.

The spectra from blank samples did not bring any ^{13}C NMR signals. The proton NMR spectrum of CO/Pt/CaL at 7.05 T was not different from those of CO/Pt/alumina or CO/Pd/silica samples which had a weak broad resonance signal.

Table 2. Peak area data of the annealed samples[†]

M_1	CO/Pt/BaL sample (%)	CO/Pt/CaL sample (%)
340±30 ppm	60±4	68±4
210±10 ppm	27±4	21±4
124±2 ppm	11±4	11±4
181±1 ppm	~15±4*	~16±4*

[†]All peaks except the one at 340±30 ppm were fitted with Lorentzian line shape. The peak area of the 340±30 ppm peak was measured from a remained broad intensity after subtraction of the peaks at 210±10 ppm and 124±2 ppm.

*This gas phase peak area in the spectra of the vacant portion of the sample tube is a relative value when the total area of three peaks at 340, 210, and 124 ppm is 100%.

Discussion

Overall, the broad peak is similar to that studied in our previous work on highly dispersed CO/Pt/silica or CO/Pt/alumina samples.[1] In both cases, the same overall linewidth, a homogeneous linewidth measured by T_2 much narrower than the observed MAS or static one, ineffectiveness of MAS and TOSS, disappearance of the broad peak in PASS were observed. In addition, no shape change of a hole upon τ_D variation, a hole relaxing at the same rate with T_1, field independent spectrum and T_1 relaxation, multiexponential T_1 behavior, and T_1 anisotropy over the resonance region are detected for both cases. The principal difference is M_1 values which are 230±30 ppm for the CO/Pt in the zeolite samples and 340±40 ppm for the silica or alumina supported CO/Pt samples. M_1 values for the CO/Pt in the zeolite samples, 230±30 ppm (present work) or 210±23 ppm (reported by Sharma *et al.* in ref. 15), may be the smallest observed M_1 values among reported ones for ^{13}CO bound to Pt particles to date. The M_1 of ^{13}C NMR spectra of CO bound Pt particles on silica or alumina has been independent of dispersion of the Pt particles up to 0.96.[1,12] IR spectroscopic results indicate that CO molecules are adsorbed on Pt particles in L-zeolite as in CO/Pt/alumina or CO/Pt/silica samples.[15,17c and d] Only a very small amount (about <7%) of CO bound to Pt particles in the L-zeolites can be attributed to bridging CO for our samples on the basis of the IR results.[17c] Therefore, the broad peak in the spectra is assigned mostly to linear CO bound to Pt particles in the L-zeolites. In contrast, Sharma *et al.'s* IR results[15] show a large amount of bridging CO and they assigned 50±3% for linear CO, 36±4% for bridging CO, and 14±2% for CO on Pt particles outside of the L-zeolite channels. They observed that the linear CO peak was narrowed by 2.6 kHz MAS giving 168 and 157 ppm isotropic peaks while the bridging component was not affected. Although M_1 values (210±25 ppm for theirs and 230±30 ppm for ours) and static line shapes are similar, our CO/Pt/particles in L-zeolite channels are suggested to be different from theirs on the basis of differences in MAS spectra, average T_1 (2.1 s for theirs and 218 ms for ours), and IR spectra.

The disappearance of the broad peak in the PASS of either CO/Pt/alumina or the CO/Pt/L-zeolites supports the existence of a distribution of isotropic peaks with some spinning side bands for individual isotropic peaks. The PASS pulse sequence is used to make all odd number of spinning sidebands 180 degree out of phase with all even order spinning side bands and it does not have inherent signal loss like the TOSS sequence. Therefore, the PASS spectrum would be the same with the MAS spectrum if the broad component consisted solely of a distribution of isotropic peaks with no shift-like anisotropy. On the other hand, if the broad line has a significant component of its width due to a shift-like anisotropy such as chemical or Knight shift anisotropy and bulk magnetic susceptibility broadening, a group of well resolved odd order spinning side bands about an isotropic peak are expected to appear 180 degree out of phase with the even order sidebands. Thus, our PASS spectrum can be explained with the case that odd spinning sidebands cancel out even spinning sidebands and isotropic peaks due to overlapped inherent broader static linewidth of each isotropic peak than the spinning rate employed. The distribution of isotropic peaks implies that the surface of the Pt particles has various sites for CO binding. The distribution range of the isotropic peaks can be correlated with the widths of the TOSS spectra while the MAS linewidths of individual isotropic peaks can be correlated with the T_2 values. Consequently, the number of the CO binding sites with different isotropic chemical shifts is presumed to be many.

The difference of the M_1 values may be explained by several factors. The difference of the size and shape of Pt particles in L-zeolites and on silica or alumina could be a reason. The Pt particles supported on alumina or silica have been assumed to have a cuboctahedral shape.[5] However, when the Pt particle is smaller and located in a confined space such as inside of a channel, as in L-zeolite, it is not necessarily expected to keep the same shape. A contacting area of a Pt particle on supports is expected to vary accordingly when Pt particle shape changes. As a result, the surface sites on the Pt particles supported on alumina or silica could be overall more metallic than those of the particles in L-zeolites and have greater Knight shift. Unfortunately, it is difficult to distinguish Pt particle shapes by the NMR spectroscopy. Alternatively one could invoke metal-support interactions. It is expected to produce downfield shift of the ^{13}C peak if electron transfer from basic L-zeolite to Pt particle is considered. However, it is opposite to our observation. In addition, there was no noticeable change in the NMR spectra according to differences of exchanged cations, which was expected in the presence of strong metal-support interactions. Relative intensities for the 124 ppm peak were initially regarded as a possible evidence for the interaction. However, these were confirmed to be random. The upfield shift of the M_1 due to a decrease of a relative population of bridging CO in a more highly dispersed Pt sample would be negligible since the amount of bridging CO even in a low dispersion sample was observed less than 7% and similar in all samples by IR.[17c and d] If CO spends some time on the surface of supports as well as on the surface of Pt particles, the M_1 is expected to be upfield shifted by the amount depending on the relative population of CO on support surfaces. This equilibrium concentrations of CO on metallic and nonmetallic sites are expected to be functions of temperature. However, the NMR spectrum taken at 80±3 K had the same M_1 value as the room temperature spectrum, which implies there was no shifting of the equilibrium concentration of CO from nonmetallic to metallic sites or *vice versa* at low temperature. In addition, the IR spectroscopic result showed CO bound to Pt particles,[17c] but not on the oxide support. Therefore, the explanation by spillover of CO to support is unlikely. A reduction in the susceptibility of the metal particles by adsorbed hydrogen during the reactivation process does not seem to be a proper explanation either, since all other samples were prepared using a similar procedure with the high temperature treatment under hydrogen as a final step before CO adsorption.[1,12] It is unlikely that more hydrogen remains on the Pt particles in L-zeolite than on alumina or silica. Proton NMR shows no difference between alumina or silica supported and L-zeolite supported samples. However, the possibility can not be excluded that traces of hydrogen under the NMR detection limit exist in some of the samples.

It is also possible that Pt particles in the L-zeolite were not fully reduced due to lower reduction temperatures than those for the alumina or silica supported samples.[31]

The T_1 relaxation curves taken at both 7.05 and 11.7 T magnetic field strengths were the same (Figure 5) and the relaxations were faster than typical for a diamagnetic sample. The line shape has a wider width for a typical diamagnetic sample also. These results suggest that the main spin lattice relaxation mechanism could be due to the interaction with conduction electrons although the average shift is closer to a diamagnetic one. Also the line shape close to Gaussian shape rather than a well-defined powder pattern and ineffectiveness of MAS to narrow the linewidth suggest that all these observations are due to magnetic susceptibility of metallic Pt particles.[10] The smaller T_1 at more downfield-shifted resonance frequency implies more strongly than other results that T_1 relaxation is mainly due to the interaction with conduction electrons. In addition, the average T_1 is longer than that of samples supported on a alumina or silica which have greater M_1 values. Unfortunately, the average T_1 values used for comparison are obscured by the fact that the magnitudes of shift anisotropy for individual isotropic peaks are not known. However, the qualitative observation is enough at present to support a Korringa relation in L-zeolite supported Pt samples. Our T_1 data could be well fitted with more than three as well as three exponential functions as Sharma *et al.'s*. Only the fact that T_1 data can be well fitted with a certain minimum number of exponentials does not necessary mean that the minimum number of exponentials is the number of different T_1 sites. Our TOSS and PASS results clearly support that there are isotropic peaks much more than three. Many shoulders observed in the CO region in the IR spectra[17c] also support existence of more than three T_1 values. Thus, multiexponential behavior of our T_1 data is due to many overlapped (more than three) T_1 components of linear CO on Pt particles.

A Korringa plot[32,33] will be used in the near future to clarify the mechanisms of the observed shift distribution. Either of two explanations is possible for the observation that the average shift is closer to a diamagnetic one although the line shape has a wider width and a faster relaxation rate than typical for a diamagnetic sample. If the Knight shift contributions from both the Fermi contact and orbital terms of hyperfine interaction with conduction electrons[5] are small, non-Korringa relaxation will be observed. On the other hand, if the average shift is small because these two terms cancel each other due to opposite signs, the Korringa relation will hold. However, the Korringa constant obtained from the plot will not match with the observed average Knight shift.

The representative spectra of the annealed samples are composed of a broad asymmetric peak with a center of gravity at 340 ± 30 ppm, a Lorentzian peak at 210 ± 20 ppm, and a sharp Lorentzian peak at 124 ± 2 ppm. The broad resonance component at 340 ± 30 ppm has similar T_1 and T_2 relaxation rates, linewidth, and resonance position to the spectrum of highly dispersed (80-96%) CO/Pt/silica or CO/Pt/alumina samples.[1,12] Therefore, this 340 ± 30 ppm peak is assigned to CO linearly bound to the Pt particles outside of the L-zeolite channels; in similar sizes and shapes to the ones on alumina or silica. The outer surface of the L-zeolites is not different from silica while the inner surface of the zeolite is influenced by metal cations or protons in the channel of the zeolite. Irreversible M_1 shift of the broad component from 230 ± 30 ppm to 340 ± 30 ppm upon annealing suggests that most of Pt particles in the zeolite channels were agglomerated resulting in bigger Pt particles on the outer surface. This agglomeration of Pt particles brings inevitably the reduction of the number of CO adsorption sites so that CO desorption is expected to occur from samples of saturated CO coverage. The peak at 210 ± 20 ppm is assigned to physisorbed CO on the zeolite exchanging with gas phase CO on the basis of the following observation. Desorbed gas phase CO was detected as a peak at 181 ± 1 ppm with a FWHH of ~850 Hz from the vacant part of the sample tube (Figure 8A) while this 181 ± 1 ppm peak was not observed from the part filled with the sample (not shown). Both the 210 ± 10 (Figure 6B) and 181 ± 1 ppm peaks (Figure 8A) were relatively narrow at room temperature and broadened in the low temperature spectrum.

Much easier desorption of CO from Pt/L-zeolite samples, agglomeration of the Pt particles, and smaller M_1 of the spectra suggest that initial adsorption sites on Pt in the L-zeolite channels have different characters from those on Pt/alumina or Pt/silica. The average size of L-zeolite supported Pt particles was similar to that of alumina or silica supported Pt particles measured either by EXAFS or by chemisorption. The possible explanation for the different characters would be that the shape of Pt particles and/or ordering of Pt atoms in a particle should differ unless the little difference in the average Pt particle sizes not detected by chemisorption is the cause.

Carbon-13 NMR spectra of CO on silica or alumina supported Pt particles were independent of dispersion while CO on supported Pd or Ru were dependent on dispersion. Highly dispersed Rh or Ru samples have multiple carbonyls on single atoms or ions as well as CO on metal particles.[6] As a result, Rh and Ru samples lose metallic character at a similar dispersion to our Pt in L-zeolite samples resulting in smaller M_1 and longer T_1 relaxation times.[6,7] Pd samples were observed to have a greater average Knight shift, easier CO diffusion and more bridging CO on the bigger Pd particles, which was explained by less availability of electron-deficient edge or corner sites for the bigger Pd particles.[2] When the Pd particles were smaller, smaller Knight shifts and mobility reduction of CO on the surface of the Pd particles were observed due to tighter binding of CO at more available edge or corner sites in a linear fashion.[2,14] On the other hand, the ^{13}C NMR result of CO on Pt particles can primarily be explained by the following differences compared with supported Pd or Rh or Ru samples. Carbon monoxide on Pt particles is predominantly in a linear form regardless of dispersion and does not diffuse as easily on Pd at a similar dispersion. Platinum would not produce ions as easily as Rh or Ru since it is much more noble than Rh or Ru. The observation on CO/Pt/alumina or CO/Pt/silica implies that ^{13}C NMR spectra of CO/Pt is predominantly governed by a local adsorption rather than by a whole Pt particle as long as Pt particle size is greater than the critical size and particle shape is well defined. In this case, differences in Pt dispersion would not produce noticeable change in ^{13}C NMR spectra. Sharma *et al.* observed much smaller M_1 value of ^{13}C spectra from CO/Pt/L-zeolite than CO/Pt/silica

or CO/Pt/alumina with similar dispersion.[15] Their results from IR spectroscopy, T_1 and M_1 measurement, and MAS led them to conclude that most of CO on Pt particles in L-zeolite channels are bridging and linear CO on *diamagnetic* Pt particles composed of 5 to 6 Pt atoms. Our Pt particles in L-zeolite channels did not show definite diamagnetic characters like theirs except the similar M_1 value close to diamagnetic ones. Although their M_1, overall line shapes of the ^{13}C NMR spectra, and the dispersions measured by chemisorption were quite similar to ours, our samples did not have long T_1 values and MAS effectiveness like theirs. Thus, our Pt particles in the L-zeolite must consist of more than 5 to 6 Pt atoms per particle. The average diameter of Pt particle estimated by EXAFS was 10-12 Å which corresponds to 30-34 Pt atoms.

Differences between Sharma *et al.'s* and our experimental results would be due to the different sample preparation methods. They used incipient wetness impregnation method after the zeolite was base-exchanged to full capacity. Our samples were made by ion exchange in acidic condition. Another different procedure is that Pt was incorporated before the L-zeolites were exchanged with M^{++} ions for our samples while theirs were prepared by exchanging with M^{++} ions prior to Pt particle formation. Moreover, our samples have higher Pt loading than theirs (about 3.5 versus about 1 weight %). These differences might have brought either different Pt particle shapes or a little bigger Pt particles in our samples although this size difference was not detected by the dispersion measured with chemisorption. It should also be pointed out that most of their data were obtained from CO/Pt/KL while ours from CO/Pt/ML where M stands for Ba, Ca, or Mg. According to their observation and argument, our CO/Pt/ML samples are expected to have improved stability of small Pt particles in zeolite channels or suppressed formation of large Pt particles on the outer surface of the zeolite, and more linear CO population than their CO/Pt/KL samples. Our observation agrees with this expectation qualitatively. However, it should be pointed out that the Pt particles in the channels are not necessarily smaller in the ML than in the KL contrary to their argument.

The 124 ppm is tentatively assigned to CO_2 bouncing off the inner walls of the L-zeolites.[34] No detection of this 124 ppm peak from the vacant part of the sample tubes implies that CO_2 spends more time as physisorbed species on the surfaces of L-zeolite than as a gas phase CO_2. A holeburning experiment at this peak shows that no exchange of this component with the ^{13}CO adsorbed on Pt particles occurs on the T_1 relaxation time scale. In addition, the relaxation times of this peak does not change after annealing.

Conclusion

Static and MAS NMR spectroscopic techniques were employed to investigate ^{13}CO chemisorbed on platinum particles in L-zeolites. The sharp symmetric peak at 124 ± 2 ppm is assigned to CO_2 spending most of its time as physisorbed on the inner surfaces of L-zeolites. The broad asymmetric peak at 230 ± 30 ppm in the spectra is assigned to CO linearly bound to Pt particles in the L-zeolites. This linearly bound CO was observed to have a wide distribution of isotropic shifts from bonding site to bonding site, which is similar to our previous results of highly dispersed (80-96%) CO/Pt/silica or CO/Pt/alumina samples. But the first moment value was smaller than those of highly dispersed (80-96%) CO/Pt/silica or CO/Pt/alumina samples. Another difference is that CO was easily desorbed from Pt particles in the L-zeolite upon annealing. Agglomeration of Pt particles also was observed after annealing. Thus, locating Pt particles in the L-zeolite channels was not necessarily enough to produce small *diamagnetic* particles although it was good enough to create small Pt particles collectively different from CO/Pt/alumina or CO/Pt/silica samples in terms of particle shape and/or ordering of Pt atoms in a particle. The characters of Pt particles in the L-zeolite seem to be strongly governed by sample preparation methods, metal loading, sample treatment temperature. Comparison of our observation on CO/Pt/L-zeolite with Sharma *et al.'s* reveals that the properties of Pt particles can be dramatically different even when the static NMR spectra and the dispersion measured by chemisorption are similar. Their Pt particles in the L-zeolite channels were diamagnetic and ours were not. Our results indicate that in order to interpret data of *highly dispersed samples* reliably, it is essential to take advantage of the strengths of several techniques together-first moment and relaxation time measurement from wideline NMR, detection of isotropic and anisotropic line broadening with MAS and TOSS, average particle size determination by EXAFS, relative population measurement of linear CO and bridging CO by IR.

Acknowledgement. Acknowledgement is made to the Donors of the Petroleum Research Fund, administered by the American Chemical Society. Partial supports by National Science Foundation and by MOST (Ministry of Science and Technology in Korea) are also acknowledged.

References

1. Zilm, K. W.; Bonneviot, L.; Hamilton, D. M.; Gretchen, W. G.; Haller, G. L. *J. Phys. Chem.* **1990**, *94*, 1463.
2. Zilm, K. W.; Bonneviot, L.; Haller, G. L.; Han, O. H.; Kermarec, M. *J. Phys. Chem.* **1990**, *94*, 8495.
3. Rudaz. S. L.; Ansermet, J.-P.; Wang, P.-K.; Slichter, C. P.; Sinfelt, J. H. *Phys. Rev. Lett.* **1985**, *55*, 2731.
4. Ansermet, J.-P.; Slichter, C. P.; Sinfelt, J. H. *J. Chem. Phys.* **1988**, *88*, 5963.
5. Ansermet, J.-P.; Wang, P.-K.; Slichter, C. P.; Sinfelt, J. H. *Phys. Rev.(B)* **1988**, *37*, 1417.
6. (a) Duncan, T. M.; Root, T. W. *J. Phys. Chem.* **1988**, *92*, 4426. (b) Duncan, T. M.; Thayer, A. M.; Root, T. W. *Phys. Rev. Lett.* **1989**, *63*, 62.
7. (a) Duncan, T. M.; Zilm, K. W.; Hamilton, D. M.; Root, T. W. *J. Phys. Chem.* **1989**, *93*, 2583. (b) Duncan, T. M.; Yates Jr., J. T.; Vaughan, R. W. *J. Chem. Phys.* **1980**, *73*, 975.
8. Slichter, C. P. *Ann. Rev. Phys. Chem.* **1986**, *37*, 25.
9. Wang, P.-K., Ansermet, J.-P., Rudaz, S. L.; Wang, Z.; Shore, S.; Slichter, C. P.; Sinfelt, J. H. *Science* **1986**, *234*, 35.
10. Duncan, T. M. *Colloids Surf.* **1990**, *45*, 11.
11. Ansermet, J.-P. *Ph. D. Thesis*, University of lllinois, Urbana-Champaign, IL, 1985.
12. Rudaz, S. L. Ph. D. Thesis, University of lllinois,

Urbana-Champaign, IL, 1984.
13. Wang, P.-K.; Ansermet, J.-P.; Slichter, C. P.; Sinfelt, J. H. *Phys. Rev. Lett.* **1985**, *55*, 2731.
14. Bradley, J. S.; Millar, J.; Hill, E. W.; Melchior, M. *J. Chem. Soc. Chem. Commun.* **1990**, 705.
15. Sharma, S. B.; Laska, T. E.; Balaraman, P.; Root, T. W., Dumesic, J. A. *J. of Catal.* **1994**, *150*, 225.
16. Takaish, T. *J. Chem. Soc., Farday Trans. I* **1988**, *84*, 2967.
17. (a) Larsen, G.; Haller, G. L. *Catal. Letters* **1989**, *3*, 103. (b) McHugh, B. J.; Larsen, G. L. *J. Phys. Chem.* **1990**, **94**, 8621. (c) Larsen, G.; Haller, G. L. In *Catalytic Sci. and Technol.*; Yoshida, S. et al Eds; Kodansha Ltd.: Tokyo, 1991, Vol.1, p.135. (d) Sheppard, N.,; Nguyen, T. T. In *Advances in Infrared and Raman Spectroscopy*; Clark, R. J. H., Hester, R. E. Eds.; Heyden, London, 1978.
18. Parra, C. F.; Ballivet, D.; Barthomeuf, D. *J. Catal.* **1975**, *40*, 52.
19. Umansky, B. S.; Hall, W. K. *J. Catal.* **1990**, *124*, 97.
20. Gay, I. D. *J. Magn. Reson.* **1984**, *58*, 413.
21. Stejskal, E. O.; Schaefer, J. *J. Magn. Reson.* **1974**, *14*, 160.
22. Maricq, M. M.; Waugh, J. S. *J. Chem. Phys.* **1979**, *70*, 3300.
23. Olejniczak, E. T.; Vega, S.; Griffin, R. G. *J. Chem. Phys.* **1984**, *81*, 4804.
24. Mehring, M. *Principles of High Resolution NMR in Solids* 2nd Edition; Springer-Verlag: Berlin, Heidelberg, New York, 1983, p 304.
25. Morris, G. A.; Freeman, R. *J. Magn.* **1978**, *29*, 433.
26. Duncan, T. M.; Thayer, A. M.; Root, T. W. *J. Chem. Phys.* **1990**, *92*, 2663.
27. (a) Dixon, W. T. *J. Chem. Phys.* **1982**, *77*, 1800. (b) Dixon, W.T.; Schaefer, J.; Sefcik, M. D.; Stejskeal, E. O.; Mckay, R. A. *J. Magn. Reson.* **1982**, *49*, 341.
28. Raleigh, D. P.; Olejniczak, E. T.; Vaga, S.; Griffin, R. G. *J. Magn. Reson.* **1987**, *72*, 238.
29. Raleigh, D. P.; Olejniczak, E. T.; Griffin, R. G. *J. Chem. Phys.* **1988**, *89*, 1333.
30. Raleigh, D. P.; Olejniczak, E. T.; Vega, S.; Griffin, R. G. *J. Am. Chem. Soc.* **1984**, *106*, 8302.
31. Maesen, T. L. M.; Botman, M. J. P.; Slaghek, T. M.; She, L.-Q.; Zhang, J. Y.; Ponec, V. *Appl. Catal.* **1986**, *25*, 35.
32. Abragam, A. *The Principles of Nuclear Magnetism*; Oxford Univ. Press: New York, 1961.
33. Slichter, C. P. *Principles of Magnetic Resonance* Third Edition; Springer-Verlag: New York, Berlin, Heidelberg, 1990.
34. Stejskal, E. O.; Schaefer, J.; Henis, J. M. S.; Tripod, M. K. *J. Chem. Phys.* **1997**, *61*, 2351.

Reconstruction of Pd Particles Supported on Silica in the Presence of CO as Studied by Carbon-13 NMR

Oc Hee Han*, Gary L. Haller†, and Kurt W. Zilm†

Magnetic Resonance Research Group, Korea Basic Science Institute, Taejon 305-333, Korea
†Departments of Chemistry and †Chemical Engineering, Yale University, New Haven, Connecticut 06511, USA
Received March 12, 1998

The ^{13}C NMR spectrum of ^{13}CO adsorbed on Pd particles varies dramatically depending on dispersion. The spectrum of highly dispersed Pd particles supported on silica is a powder pattern ~800 ppm wide with a first moment of 410 ppm. A low dispersion sample has a motionally narrowed line centered at 750±10 ppm and only ~85 ppm full width at half height (FWHH). Over several years, high dispersion samples show an increase in the intensity near 750 ppm. These observations are interpreted as an increase of *mobile bridging* CO on high dispersion Pd surfaces of particles which resulted from smoothing of the metal particle surfaces in the presence of CO.

Introduction

The structure and surface chemistry of noble metal particles (Pt, Pd, Rh, Ru, etc.) supported on high surface area oxides have received a great deal of attention due to their wide application as catalysts in many technologically important reactions (CO oxidation, water gas shift reaction, hydrogenation, etc.).[1] One of the model systems most extensively studied is CO adsorbed on such supported metal particles, and the results of these studies have formed the basis of the most widely accepted models of molecular chemisorption for many reasons. CO is for example an important reactant in the chemistry of the Fischer-Tropsch processes[2] and binds tightly to the majority of interesting catalytic metal surfaces[2-6] at ambient temperature. In addition, CO is implicated in the surface reconstruction or reforming of metal particles under certain conditions.[7-28] Thus, the study of the interaction of CO with supported metal particles has relevance to nearly

*Author to whom all correspondence should be addressed.